High-Index Materials for UV Lithography Optics

John H. Burnett,
Physics Laboratory, NIST, Gaithersburg, MD 20899
john.burnett@nist.gov

Abstract: A survey of candidate high-index lens materials for UV lithography optics is presented. These materials may enable extension of 193 nm immersion lithography to smaller feature sizes, while reducing lens system sizes.
OCIS codes: (160.4670) Optical materials; (160.4760) Optical properties.

1. Introduction

Optical designers exploit the diversity of refractive indices and wavelength dispersions of various available lens materials to optimize performance and minimize aberrations. In the visible, at least 50 different common glass types are available to choose from. As the design wavelength gets shorter, the choices become more restricted. Presently the semiconductor lithography industry uses 193 nm excimer laser radiation to take advantage of the diffraction-limited resolution gain at shorter wavelengths. At this wavelength the choice of high-quality commercial lens materials comes down to just two, UV fused silica and calcium fluoride, and the indices for both of these materials are relatively low (1.56 for fused silica and 1.50 for calcium fluoride [1].) This puts severe constraints on optical system design.

Over the past several years the semiconductor lithography industry has pursued an approach to extend the resolution capabilities of 193 nm lithography by including an immersion fluid between the final lens element and the photosensitive resist coated silicon wafer. This takes advantage of the index factor n in the Rayleigh imaging resolution formula, $\mathrm{Res}_{\mathrm{min}} = k_1\,\lambda/(n\sin\theta)$, where λ is the illumination wavelength, θ is the half angle of the largest-angle rays at the focal point, n is refractive index at the focal point, and the prefactor k_1 has a theoretical limiting value of 0.25. With k_1 pushed to practical limits and the wavelength fixed at 193 nm, the resolution limit of the aerial image is determined by the numerical aperture (NA= $n\sin\theta$). For plane-parallel resist-fluid and fluid-lens interfaces, the NA is limited by the lowest refractive index of the resist, the immersion fluid, and the final lens element: $\mathrm{NA} \le \min(n^{\mathrm{resist}}, ,n^{\mathrm{fluid}}, n^{\mathrm{lens}})$ (See Fig. 1.) The first-generation 193 nm immersion lithography systems are expected to use water, with a 193 nm index of 1.44, as the immersion fluid, and this is the lowest index of the three. Future-generation immersion systems are expected to use fluids with indices as least 1.66 [2]. For these systems the index of the final lens element will be the bottleneck for increased resolution.

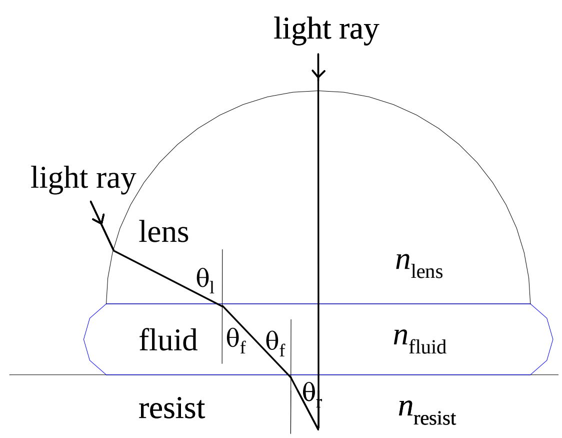

Fig. 1. Schematic of light rays traveling through final lens element, immersion fluid, and resist. The NA is limited by the smallest index.

A further interest in the availability high-index lens materials is motivated by their impact on lens system size. As the value of NA/n increases, the lens system diameter increases to contain aberrations. State-of-the-art 193 nm dry and immersion system designs have NA/n > 0.9, and the resulting lens system sizes are approaching practical limits. However, models have demonstrated that by incorporation of high index materials (n ≥ 1.7), lens system diameters could be significantly reduced, enabling NA ≥ 1.65 immersion systems with practical lens sizes.

2. High-Index Materials

To be of use for 193 nm lithography optics, a high-index material would have to meet certain requirements. First, the material would have to be transparent at this wavelength, requiring that the material have an intrinsic band gap of at least 6.41 eV. Second, the material would have to have isotropic optical properties, so either have cubic crystalline structure or be amorphous or polycrystalline. Finally, the index must be large enough to make it worth the effort to develop the material. The industry has set a high index material minimum specification of about 1.7. There are two types of materials that have the possibility of obeying the transmission requirements, the halides and the oxides. Impractically high hygroscopicity rules out the halides except for the fluorides. The fluorides however generally have indices smaller than the requirement because of the relatively low polarizability of strong fluoride bond. With the highly polarizable oxygen bond, the 193 nm transmitting oxides generally have indices close 2.0. Consequently the search focused primarily on the oxides.

There are over 500 common oxide materials and over 50 common fluoride materials, for example those tabulated with their visible properties by Shannon, *et al.* [3]. Their UV properties are generally not known. The constraint of 193 nm transmission drastically limits the possibilities. The material can only contain a certain limited set of elements. For example, it cannot contain elements with open *d* for *f* shells, which give rise to strongly absorbing UV transitions. These and other constraints reduce the practical possibilities to seven classes indicated in Table 1.

Table 1. High Index Materials Candidates

Materials Type	Key properties
$BaLiF_3$	low index (1.64), good UV quality, marginal IBR (25 nm/cm)
Simple Oxides	
type: MgO, CaO,…	high index (~2.0), high melting point, high IBR (>50 nm/cm)
Aluminates	
spinel ($MgAl_2O_4$, $ZnAl_2O_4$)	high index (~2.0), good UV quality, high IBR (>50 nm/cm)
ceramic $MgAl_2O_4$	high index (~2.0), poor UV quality, negligible IBR
Garnets	
type: $X^{(+3)}{}_3Y^{(+3)}{}_5O^{(-2)}{}_{12}$ ($Lu_3Al_5O_{12}$)	high index (~2.0), good UV quality, marginal IBR (~30 nm/cm)
type: $X^{(+2)}{}_3Y^{(+3)}{}_2Si^{(+4)}{}_3O^{(-2)}{}_{12}$ (X=Mg,Ca)	high index (~2.0), difficult to grow, low IBR (<10 nm/cm)
type: $X^{(+2)}{}_3Y^{(+3)}{}_2Ge^{(+4)}{}_3O^{(-2)}{}_{12}$ (X=Mg,Ca)	high index (~2.0), marginal UV quality, marginal IBR

Though a number of high-index material possibilities were identified, the project unexpectedly ran into a serious challenge: the high intrinsic birefringence (IBR) of high-index materials. IBR is a symmetry-breaking effect in cubic crystals caused by the finite value of the photon momentum at short wavelengths (spatial dispersion.) It results in index anisotropy and birefringence in cubic crystals which would otherwise be absent by symmetry. The effect was first discussed by H. A. Lorentz in 1878 [4], but being very small was not considered to have any practical effect. This was until it was identified in calcium fluoride in the UV and shown to have a major implications for proposed 193 nm and 157 nm optical lithography technologies [5,6]. For calcium fluoride, with an IBR value at 193 nm of –3.4 nm/cm, it was demonstrated that the effect could be designed around by judiciously orienting the relative crystal axes of different optical elements for cancellation effects. However, the job becomes much more difficult for larger IBR values. The problem for high-index materials is illustrated in Fig. 2, which demonstrates a trend of increasing IBR with index. Both increase as the absorbing band edge gets closer to the 193 nm photon energy. The result is that all high-index crystalline fluoride and oxide materials measured so far have IBR values substantially larger than that of calcium fluoride, and correction has been difficult even for the calcium fluoride value. The lithography industry has established a specification of 10 nm/cm for the largest tolerable IBR value.

Ceramic spinel (see Table 1.) has effectively no IBR, due to the random orientation of the crystalline domains, which wash out the effect. However, the UV properties are poor. None of the crystalline candidates comes close to satisfying the minimum specification, except possibly for the garnets. Fig. 2. shows that the garnets $Y_3Al_5O_{12}$ (YAG) and $Lu_3Al_5O_{12}$ (LuAG) have IBR values, that while higher than specifications, appear to fall well below the trend curve. This is probably due to the unique crystal structure of these materials. The garnet crystal structure has 4 formula units (80 atoms) per primitive cell. Each cation is surrounded by oxygen cages with different orientations. This gives rise to cancellation effects and results in relatively low IBR. Further, the IBR effect has a sign, and miscible materials with opposite signs can be combined to null out the effect [6]. Since the garnet structure is stable for a large variety cations, there is a possibility of the existence of garnets with acceptable values. As a result, the project has focused on the garnets. The project has grown and characterized over 15 different types of promising garnets. Several of the silicate and germanate garnets (see Table 1.) appear to have the requisite properties.

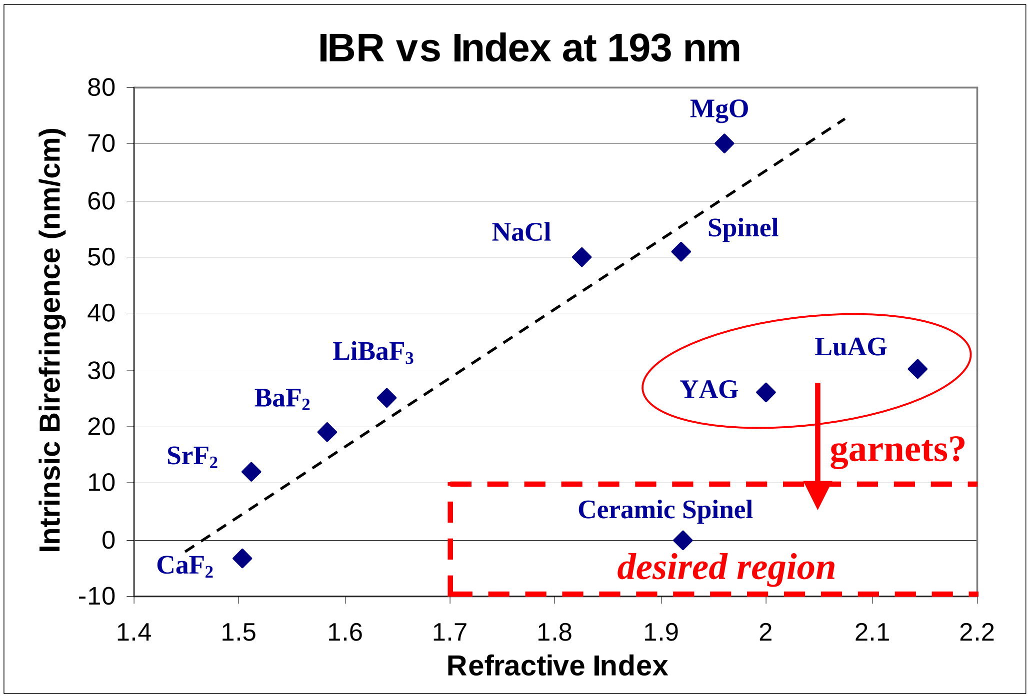

Fig. 2. IBR versus refractive index at 193 nm.

3. Conclusions

A project is underway to identify and characterize UV-transmitting high-index materials that could be useful for precision UV optics design. In particular, such materials could enable extension of the capabilities of state-of-the-art 193 nm lithography. One class of materials, the garnets, appear particularly promising, and the project has been exploring the compositional parameter space of these materials. Several of these appear to be credible candidates.

[1] Rajeev Gupta, John H. Burnett, Ulf Griesmann, and Matthew Walhout, "Absolute refractive indices and thermal coefficients of fused silica and calcium fluoride near 193 nm," Applied Optics **37**, pp. 5964-5968 (1998).
[2] R. H. French, H. Sewell, M. K. Yang, S. Peng, D. McCafferty, W. Qiu, R. C. Wheland, M. F. Lemon, L. Markoya, and M. K. Crawford, "Imaging of 32-nm 1:1 lines and spaces using 193-nm immersion interference lithography with second-generation immersion fluids to achieve a numerical aperture of 1.5 and a k_1 of 0.25," J. Microlith., Microfab., Microsyst. **4**, 031103-1 to 031103-14 (2005).
[3] R.D. Shannon, R.C. Shannon, O. Medenbach, and R.X. Fischer, "Refractive Index and Dispersion of Fluorides and Ooxides," J. Phys. Chem. Ref. Data, Vol. 31, 931-970 (2002).
[4] H. A. Lorentz, *Collected Papers II*, (Martinus Nijohff, The Hague, 1936), pp. 1-119, esp. p. 79; originally *Verh. Kon. Akad. Wetensch*, **18** (1878).
[5] John H. Burnett, Zachary H. Levine, and Eric L. Shirley, "Intrinsic birefringence in calcium fluoride and barium fluoride," Phys. Rev. B **64**, 241102 (2001).
[6] John H. Burnett, Zachary H. Levine, Eric L. Shirley, and John H. Bruning, "Symmetry of spatial-dispersion-induced birefringence and its implications for CaF_2 ultraviolet optics," Journal of Microlithography, Microfabrication, and Microsystems **1**, pp. 213-224 (2002).